New Methods for *ALK* Status Diagnosis in Non–Small-Cell Lung Cancer

An Improved ALK Immunohistochemical Assay and a New, Brightfield, Dual ALK IHC–In Situ Hybridization Assay

Hiroaki Nitta, PhD, MBA, Koji Tsuta, MD, PhD,† Akihiko Yoshida, MD, PhD,† Steffan N. Ho, MD, PhD,‡ Brian D. Kelly, PhD,* Lauren B. Murata, PhD,* Jerry Kosmeder, PhD,* Katie White, PhD,* Sandra Ehser, PhD,§ Penny Towne, MBA,* Crystal Schemp, MPH,* Abigail McElhinny, PhD,* Jim Ranger-Moore, PhD,* Chris Bieniarz, PhD,* Shalini Singh, MD,* Hitoshi Tsuda, MD, PhD,† and Thomas M. Grogan, MD**

Introduction: The demonstration of anaplastic lymphoma kinase (ALK) positivity in non–small-cell lung cancer (NSCLC) has been hindered by the technical complexity and interpretative challenges of fluorescence in situ hybridization methods for detection of *ALK* gene rearrangement and by the inadequate sensitivity of existing immunohistochemistry (IHC) methods for ALK protein detection. In this study, we sought to increase the sensitivity of ALK IHC detection and to develop a brightfield assay for concurrent detection of ALK protein expression and *ALK* gene rearrangement.

Methods: We developed a horseradish peroxidase–based IHC detection system using the novel, nonendogenous hapten 3-hydroxy-2-quinoxaline (HQ) and tyramide. We also developed a dual gene protein ALK assay combining a brightfield break-apart in situ hybridization *ALK* assay with another sensitive IHC method using the novel, nonendogenous hapten 5-nitro-3-pyrazole. We examined the sensitivity and accuracy of these methods using surgically resected NSCLC cases examined with *ALK* fluorescence in situ hybridization.

Results: The new HQ-tyramide IHC detection system offered readily interpretable staining with substantially greater sensitivity than conventional ALK IHC, and produced heterogeneous and homogeneous patterns of ALK protein staining among *ALK*-positive NSCLC surgical cases. The new 5-nitro-3-pyrazole–based IHC detection system was similar in ALK detection sensitivity to the HQ-tyramide IHC system and was compatible with the brightfield in situ hybridization assay.

Conclusion: The new HQ-tyramide IHC reagent system allows more sensitive assessment of ALK protein status in NSCLC cases. The new ALK gene-protein assay allows the concurrent visualization of *ALK* gene and ALK protein status in single cells, allowing more accurate ALK status determination even in heterogeneous specimens.

Key Words: ALK, Brightfield, Immunohistochemistry, In situ hybridization, Non–small-cell lung cancer.

(*J Thorac Oncol.* 2013;8: 1019-1031)

The implementation of personalized health care in cancer relies on the identification and characterization of cancer biomarkers and the availability of accurate detection systems and therapies for those biomarkers. For example, the human epidermal growth factor receptor 2 gene (*HER2*) and protein are well-established biomarkers for identifying those breast[1] and gastric cancer[2] patients who are most likely to respond to trastuzumab therapy.

Anaplastic lymphoma kinase (ALK), a tyrosine kinase, is a more recently characterized cancer biomarker[3]; in non–small-cell lung cancer (NSCLC), the presence of oncogenic *ALK* gene rearrangement leading to fusion of the *ALK* gene with any of several other specific genes is linked both to ALK protein overexpression and a dramatic therapeutic response to specific ALK inhibitors[4] such as crizotinib (Pfizer, Inc., New York, NY), which has been approved for use in *ALK*-positive, locally advanced or metastatic NSCLC.[5] To identify NSCLC patients with *ALK* gene rearrangement in clinical trials, researchers have used a break-apart fluorescence in situ hybridization (FISH) assay.[5] However, the *ALK* FISH assay is fraught with technical challenges, including FISH signal instability and scoring difficulties.[6–8]

An alternative method for determining ALK diagnostic status in NSCLC is to identify ALK protein overexpression

*Ventana Medical Systems, Inc., Tucson, AZ; †National Cancer Center Hospital, Tokyo, Japan; ‡Pfizer, Inc., La Jolla, CA; and §42 Life Sciences GmbH & Co., Bremerhaven, Germany.

Disclosure: Dr. Nitta, Dr. Kelly, Dr. Murata, Dr. Kosmeder, Dr. White, Penny Towne, Crystal Schemp, Dr. McElhinny, Dr. Ranger-Moore, Dr. Bieniarz, Dr. Singh, and Dr. Grogan are employees of Ventana Medical Systems, Inc., a member of the Roche group. Dr. Ho is an employee of Pfizer, Inc. Dr. Ehser is an employee of 42 Life Sciences. All other authors declare no conflict of interest.

Address for Correspondence: Hiroaki Nitta, PhD, Medical and Scientific Affairs, Ventana Medical Systems, Inc., 1910 E. Innovation Park Drive, Tucson, AZ 85755. E-mail: hiro.nitta@ventana.roche.com

ISSN: 1556-0864/13/0808-1019

using immunohistochemical (IHC) methods. However, the sensitive and reproducible detection of ALK by these methods presents a significant challenge because the differential expression of ALK protein occurs at a low level.[6] Although a multiplex reverse transcription–polymerase chain reaction (RT-PCR)–based assay can sensitively detect certain *ALK* fusion-gene variants,[7,9] reproducible RT-PCR results are technically difficult to obtain in formalin-fixed, paraffin-embedded (FFPE) tissue sections.[6,10] The various advantages and disadvantages of current ALK testing methodologies have led the Japanese Lung Cancer Society to recommend that multiple ALK tests should be used when an NSCLC patient is evaluated for anti-ALK therapy.[11]

The present report describes the successful development and evaluation of two new methodologies for the assessment of ALK status in FFPE NSCLC tissue. To improve IHC assay sensitivity, we incorporated the novel, nonendogenous hapten 3-hydroxy-2-quinoxaline (HQ) and tyramide amplification into a diaminobenzidine (DAB)- and horseradish peroxidase (HRP)–based assay. The new HQ-tyramide IHC detection system proved to be very useful for detecting low levels of ALK protein expression in NSCLC.

We also developed a brightfield IHC–in situ hybridization (ISH) combination assay (gene–protein assay) for the concurrent visualization of ALK protein and *ALK* gene arrangement. To make the IHC portion of this combination assay compatible with ISH, we incorporated another novel, nonendogenous hapten [5-nitro-3-pyrazole (NP)] and a novel chromogen (fast gold) into a new alkaline phosphatase (AP)–based assay. Combined with break-apart ISH methodology, this assay allows covisualization of ALK protein expression and *ALK* gene rearrangement.

MATERIALS AND METHODS

Reagents and Antibodies

All antibodies and IHC reagents were from Ventana Medical Systems, Inc. (Tucson, AZ; "Ventana") and all chemical reagents were from Sigma (St. Louis, MO) unless stated otherwise. Polyethylene glycol (PEG) linkers were purchased from Quanta Biodesign Ltd. (Powell, OH). Polyclonal goat anti-rabbit antibodies, HRP, and AP were obtained from Roche Diagnostics (Mannheim, Germany).

NSCLC and Xenograft Specimens

Eighty surgically resected, deidentified NSCLC cases (40 *ALK*-negative and 40 *ALK*-positive FISH) were provided by the National Cancer Center Hospital (Tokyo, Japan) after the study protocol was approved by the National Cancer Center Hospital Institutional Review Board. The specimens were fixed in 10% buffered formalin for 24 to 72 hours at room temperature, cut into serial, 5-mm–thick slices, and examined by eye for the presence of tumor and surrounding lung tissue. The specimens were then routinely processed for embedding in paraffin. Sections of the paraffinized tissue were cut at 4-μm thickness and mounted on Matsunami Platinum glass slides (Matsunami Glass Ind., Ltd., Osaka, Japan). Hematoxylin and eosin slides from each specimen were examined to confirm the presence of NSCLC tumor.

The *ALK* gene status of NSCLC cases was examined using the Food and Drug Administration (FDA)–approved Vysis ALK Break Apart FISH Probe Kit assay (Abbott Molecular Inc., Des Plaines, IL; hereafter, Vysis *ALK* FISH assay). For this purpose, 50 nonoverlapping tumor cells from each case were analyzed, and those cases exhibiting split-apart or lone 3′ signals in at least 15% of tumor cells were considered to be positive for *ALK* rearrangement (Table 1).

Randomly selected *ALK*-negative and -positive NSCLC cases were used to prepare two tissue microarray (TMA) blocks for assay optimization. One TMA block was prepared with *ALK*-positive NSCLC cases (14 tissue cores) whereas the other TMA block was prepared with *ALK*-negative cases (16 tissue cores). TMA slides and single-specimen–containing slides were then used in the ALK method development and assay performance studies, respectively, described herein.

The *ALK*-positive NCI-H2228 cell line (adenocarcinoma, NSCLC cells) and the *ALK*-negative A549 cell line (adenocarcinoma, human alveolar basal epithelial cancer cells) were used to produce FFPE xenograft tumors. Both xenograft tumors were embedded together in the same paraffin block. Xenograft tumor sections were used for ALK gene–protein assay development.

ALK IHC Methods

Three HRP-based IHC-detection methods (detections 1–3; Fig. 1*A*) and two AP-based IHC-detection methods (detections 4 and 5; Fig. 4*A*) were investigated for their ability to detect low-level ALK protein expression using *ALK*-positive and -negative NSCLC TMA sections. IHC staining was performed on a VENTANA BenchMark XT automated slide-processing system (Ventana), using Vysis *ALK* FISH-characterized NSCLC tissue sections. For all IHC staining, the BenchMark XT instrument heated the slides carrying the FFPE tissue sections at 65°C for 20 minutes to improve tissue adhesion and then performed the following steps: (1) deparaffinization with EZ Prep detergent solution (Ventana) (75°C; 20 minutes); (2) washing with reaction buffer; (3) ALK antigen retrieval in Cell Conditioning 1 (Ventana) (100°C; 92 minutes); (4) washing (same as step 2); (5) primary antibody (Ab) incubation with rabbit monoclonal anti-ALK Ab (clone D5F3; 36°C; 16 minutes); and (6) washing (same as step 2). All reagents used in these steps were from Ventana. All subsequent reagent incubation steps were separated by washing as in step 2.

In all three HRP-based IHC staining methods (detections 1–3), primary Ab incubation and washing were followed by secondary Ab incubation with a goat polyclonal anti-rabbit Ab. In detection 1, the secondary Ab was biotinylated, subsequently bound by a streptavidin-HRP complex, and visualized by means of a a brown precipitate produced by HRP on the addition of hydrogen peroxide and DAB. This DAB color reaction was also used in detections 2 and 3. However, in detection 2, the secondary Ab was conjugated to HQ rather than biotin, and HRP-conjugated mouse monoclonal anti-HQ Ab was used as a tertiary Ab to amplify the signal before the DAB color reaction was carried out. In detection 3, the signal was amplified even further by the addition of an HQ-tyramide complex and a second layer of HRP-conjugated

TABLE 1. *ALK* FISH Results of NSCLC Cases

	ALK FISH Result			*ALK* FISH Result	
Case Number	***ALK* Status**	**% Split[a]**	**Case Number**	***ALK* Status**	**% Split[a]**
02	Positive	42	01	Negative	6
06	Positive	27	03	Negative	9
11	Positive	72	04	Negative	5
13	Positive	36	05	Negative	6
15	Positive	48	07	Negative	4
17	Positive	36	08	Negative	6
20	Positive	44	09	Negative	2
22	Positive	53	10	Negative	2
24	Positive	32	12	Negative	2
27	Positive	44	14	Negative	2
28	Positive	56	16	Negative	6
30	Positive	50	18	Negative	6
32	Positive	48	19	Negative	3
34	Positive	40	21	Negative	2
39	Positive	35	23	Negative	10
41	Positive	72	25	Negative	10
42	Positive	56	26	Negative	10
43	Positive	76	29	Negative	5
44	Positive	40	31	Negative	4
46	Positive	46	33	Negative	3
48	Positive	52	35	Negative	5
53	Positive	64	36	Negative	7
54	Positive	16	37	Negative	2
57	Positive	54	38	Negative	3
58	Positive	40	40	Negative	5
59	Positive	50	45	Negative	0
60	Positive	52	47	Negative	0
61	Positive	28	49	Negative	7
62	Positive	30	50	Negative	3
65	Positive	58	51	Negative	4
66	Positive	46	52	Negative	3
69	Positive	48	55	Negative	7
70	Positive	50	56	Negative	1
72	Positive	52	63	Negative	6
73	Positive	65	64	Negative	4
74	Positive	56	67	Negative	2
75	Positive	32	68	Negative	0
76	Positive	46	71	Negative	8
77	Positive	47	78	Negative	4
79	Positive	50	80	Negative	4

[a]Percentage of cells exhibiting split *ALK* gene signals or lone 3′ signals.
ALK, anaplastic lymphoma kinase; FISH, fluorescence in situ hybridization; NSCLC, non–small-cell lung cancer.

mouse monoclonal anti-HQ Ab between the tertiary Ab and chromogenic reaction steps. In all three methods, the stained tissue sections were counterstained with modified Mayer's hematoxylin (Hematoxylin II; Ventana) and then incubated with Bluing Reagent (Ventana) to change the hematoxylin hue to blue. They were then dehydrated through a graded ethanol series, cleared with xylene, and cover-slipped with Tissue-Tek Film Coverslipper (Sakura Finetek Japan, Tokyo, Japan).

In the two AP-based IHC methods (detections 4 and 5), the goat polyclonal anti-rabbit secondary Ab was conjugated to NP, and the tertiary Ab was an AP-conjugated mouse monoclonal anti-NP Ab. Detections 4 and 5 differed in that the former used fast red and naphthol phosphate, a commonly used AP substrate, and the latter used fast blue BB and fast gold, a newly developed AP substrate. After counterstaining and bluing as described above, the slides were air-dried in a

conventional oven (60°C; 20 minutes) and coverslipped with Tissue-Tek Film Coverslipper.

ALK IHC slides were scanned without magnification on an Epson Artisan 700 scanner (Epson America, Inc., Long Beach, CA) using Epson Scan software (Epson America, Inc.). Micrographs were captured using an ECLPE 90i microscope (Nikon Instruments Inc., Melville, NY) equipped with a DS-Fi1 digital camera (Nikon Instruments Inc.). Captured images were prepared for figures using Adobe Photoshop CS5 (Adobe Systems Inc., San Jose, CA).

ALK Gene–Protein Assay Application

For concurrent detection of ALK protein expression and *ALK* gene rearrangement in NSCLC and xenograft tissue sections, detection 5 was used in conjunction with a brightfield break-apart ISH assay (Fig. 5*A*). FFPE NSCLC tissue sections were mounted on Matsunami Platinum slides, baked (65°C; 20 minutes), placed in the Benchmark XT instrument, and deparaffinized using EZ Prep as described above. They were then subjected to heat treatment in Cell Conditioning 1 for 92 minutes for antigen retrieval. The slides were then incubated with rabbit monoclonal anti-ALK Ab (clone D5F3; 37°C; 16 minutes), with NP-conjugated goat polyclonal antirabbit Ab (37°C; 8 minutes), and with AP-conjugated mouse monoclonal anti-NP Ab (37°C; 8 minutes). ALK IHC staining was completed using the AP substrates fast gold and fast blue BB for 8 minutes.

Brightfield *ALK* break-apart ISH methodology[12–14] was applied to ALK IHC slides with some modifications. For DNA target retrieval, the IHC-stained tissue sections were subjected to a second heat treatment in reaction buffer (90°C; 48 minutes), digested with protease (ISH-Protease 3; Ventana) (37°C; 12 minutes), and denatured (80°C; 8 minutes). A cocktail of digoxigenin (DIG)-labeled 3′ *ALK* DNA probe and 2,4-dinitrophenyl (DNP)-labeled 5′ *ALK* DNA probe was then hybridized to the tissue sections (44°C; 6 hours). Three stringency washes (72°C; 3 × 8 minutes) were performed using 2× saline soldium citrate (SSC) (Ventana). For visualization of 3′ *ALK* probe-binding sites, the tissue sections were incubated sequentially with (1) mouse monoclonal anti-DIG Ab (37°C; 20 minutes), (2) AP-conjugated goat polyclonal anti-mouse Ab for 20 minutes, and (3) naphthol and fast red, resulting in color development. The 5′ *ALK* probe-binding sites were visualized through sequential use of (1) rabbit monoclonal anti-DNP Ab (37°C; 20 minutes), (2) HRP-conjugated goat anti-rabbit Ab (20 minutes), and (3) modified HRP-Green (42 Life Sciences GmbH & Co. KG, Bremerhaven, Germany; 37°C; 16 minutes).

Stained tissue sections were lightly counterstained with diluted Mayer's hematoxylin (1:5 in water; 42 Life Sciences), dried in a conventional oven (60°C; 20 minutes), and coverslipped with a film coverslipper. Micrographs of the ALK gene–protein slides were captured as described above.

Preparation of Novel HQ and NP Reagents

First, the HQ and NP haptens (Ventana) were esterified with *N*-hydroxysuccinimide (NHS) by the following procedure: HQ- or NP-carboxylic acid (5.0 mmol, 1.0 eq) was taken up in anhydrous dichloromethane (DCM; 10 ml) in a 50-ml round-bottom flask. The solution was blanketed with anhydrous nitrogen gas (N_2), and NHS (5.5 mmol, 1.1 eq) was added followed by *N,N′*-dicyclohexylcarbodiimide (6.0 mmol, 1.2 eq, 1.0 M in DCM) and triethylamine (6.0 mmol, 1.2 eq; TEA). The reaction mixture was stirred at room temperature (RT) under N_2 for 16 hours, at which point the solvent was removed under vacuum. The residue was taken up in DCM (2 ml) and filtered to remove the urea byproduct. The resulting filter cake was washed twice with DCM (0.5 ml). The DCM washes were dried under vacuum to yield the HQ- or NP-NHS ester, which was used without further purification.

Next, the HQ and NP haptens were covalently linked to H_2N-PEG-COOH by the following procedure: the hapten-NHS ester (5.0 mmol, 1.0 eq) was taken up in DCM (10 ml) in a 50-ml round-bottom flask. The solution was blanketed with N_2, and H_2N-PEG-COOH (5.5 mmol, 1.1 eq) was added followed by TEA (6.0 mmol, 1.2 eq). The reaction mixture was stirred at RT under N_2 for 16 hours. The solvent was removed under vacuum. The residue was taken up in a minimum volume of methanol and purified by preparative HPLC. The appropriate fractions were then pooled and dried under high vacuum to give the pure NP- or HQ-PEG-COOH.

Finally, to make the HQ- and NP-PEG-NHS ester reagents, HQ- or NP-PEG-COOH (5.0 mmol, 1.0 eq) was taken up in DCM (10 ml) in a 50-ml round-bottom flask. The solution was blanketed with N_2, and NHS (5.5 mmol, 1.1 eq) was added, followed by *N,N′*-dicyclohexylcarbodiimide (6.0 mmol, 1.2 eq, 1.0 M in DCM), and TEA (6.0 mmol, 1.2 eq). The reaction mixture was stirred at RT under N_2 for 16 hours. The solvent was removed under vacuum, and the residue was taken up in DCM (2 ml) and filtered to remove the urea byproduct. The resulting filter cake was then washed twice with DCM (0.5 ml). The combined DCM washes were then dried under vacuum to yield the hapten-PEG-NHS ester, which was used without further purification.

Preparation of NP- and HQ-Conjugated PEG-Tyramides

To make HQ- and NP-conjugated PEG-tyramides, the HQ- or NP-PEG-NHS ester (5.0 mmol, 1.0 eq) was taken up in DCM (10 ml) in a 50-ml round-bottom flask. The solution was blanketed with N_2, and tyramine (7.5 mmol, 1.5 eq) was added followed by TEA (10.0 mmol, 2.0 eq). The reaction mixture was stirred at RT under N_2 for 16 hours. The solvent was removed under vacuum, and the residue was taken up in a minimal volume of methanol or DCM and purified by either preparative HPLC or automated flash chromatography. The appropriate fractions were pooled and dried under high vacuum to yield pure NP- or HQ-PEG-tyramide. The recovery typically ranged between 70% and 85%.

Preparation of NP- and HQ-Conjugated Goat Abs

To prepare the hapten-conjugated goat anti-rabbit Abs, polyclonal goat Ab in phosphate-buffered saline (pH 7.0–7.5) was treated with a solution of HQ- or NP-PEG-NHS (20 eq) in anhydrous DMSO at a final DMSO concentration less than

10% (vol/vol). Reaction mixtures were incubated for 18 hours in an amber vial at room temperature with rotation, passed through a 0.2-μm GHP syringe filter, and loaded onto a size exclusion chromatography column (Superdex 200 10/300 GL; GE Healthcare Life Sciences, Piscataway, NJ) connected to an AKTA Purifier running phosphate-buffered saline, pH 7.2, at 0.9 ml/minute. Typical yields were 70% to 80%, with 4 to 6 haptens bound per Ab.

Preparation of HRP-Conjugated Abs

To activate HRP, maleimide-PEG-NHS ester (α-maleimide-ω-NHS ester PEG; 78.8 mg, 100 eq) was mixed with 2.46 ml of HRP (61.5 mg, 1.53 μM) as a 25 mg/ml solution in 0.1 M sodium phosphate, pH 7.5. The vial was placed on an autorotator in the dark at ambient temperature (23–25°C), and the amide bond-forming reaction was allowed to proceed for 1 hour. A 400-μl aliquot was removed for purification, and the remainder of the solution was stored at 4°C. Pure HRP-PEG-maleimide was obtained by fractionation on a Superdex 200 10/300 column connected to an AKTA Purifier running 0.1 M sodium phosphate, pH 7.5, at 1.0 ml/minute. Pooling of the HRP-containing fractions yielded 2.0 ml of a 4.5 mg/ml solution of HRP-PEG-maleimide (90% recovery) as measured by ultraviolet/visible (UV/vis) spectrophotometry using an absorbance value at 280 nm (A_{280}) of 6.52 for a 1% solution (pH 6.5).

To activate the mouse anti-hapten (NP or HQ) monoclonal Abs for conjugation, each Ab (2.1 mg/ml in 0.1 M sodium phosphate, 1.0 mM ethylenediaminetetraacetic acid [EDTA], pH 6.5) was mixed with 216 μl of a freshly prepared 500 mM solution of 1,4-dithiothreitol (DTT). The vial was placed in the dark on an autorotator, and the disulfide reduction was allowed to proceed for 25 minutes. For removal of excess DTT, the reaction solution was then divided into four equal batches (because of the limited capacity of the desalting column), and each batch was passed through a PD-10 desalting column and was eluted with 0.1 M sodium phosphate, 1.0 mM EDTA, pH 6.5. The Ab-containing fractions were combined to yield 8.0 ml of a 0.8 mg/ml solution of reduced mouse anti-hapten (NP or HQ) Ab, as determined by UV/vis spectrophotometry using an A_{280} of 1.4 for a 1% solution.

To conjugate HRP to the anti-hapten Ab, the reduced Ab was added to a threefold molar excess of HRP-PEG-maleimide and incubated at ambient temperature (23–25°C) for 16 hours. The reaction mixture was passed through a Superdex 200 10/300 GL SE column to remove the unbound HRP. As determined by calculating A_{280}:A_{403}, an average of two or three HRP molecules were covalently bound to each Ab molecule. The HRP-Ab conjugates were stored at 4°C until use.

Preparation of AP-Conjugated Abs

To activate AP for conjugation to the mouse anti-hapten (HQ or NP) monoclonal Abs, it was treated with a 100-fold molar excess of maleimide-PEG-NHS ester at ambient temperature for 60 minutes. The maleimide-activated AP was then purified from the reaction mixture on a Superdex 200 10/300 GL column equilibrated with AP buffer (0.1 M Tris-HCl, 1 mM $MgCl_2$, 0.1 mM $ZnCl_2$, pH 7.5).

The mouse anti-hapten (HQ or NP) monoclonal Abs (2.1 mg/ml in 0.1 M sodium phosphate, 1.0 mM EDTA, pH 6.5) were mixed with 216 μl of a freshly prepared solution of DTT (500 mM). The vials containing the disulfide reduction reaction mixtures were placed in the dark with rotation for 25 minutes. The reaction mixtures were then split into four equal batches (because of the limited capacity of a desalting column used), and excess DTT was removed by batch-wise chromatography on a PD-10 desalting column eluted with 0.1 M sodium phosphate, 1.0 mM EDTA, pH 6.5. The Ab-containing fractions were combined to give 8.0 ml of a 0.8 mg/ml solution of purified, thiolated mouse anti-NP or -HQ Ab, as determined by UV/vis spectrophotometry.

To conjugate the activated AP to the thiolated Abs, the Abs were combined with a threefold molar excess of the maleimide-AP and incubated at ambient temperature for 16 to 18 hours. The AP-conjugated Abs were purified on a Superdex 200 10/300 GL column equilibrated with AP Buffer.

Preparation of Fast Gold AP Substrate

For fast gold synthesis, phosphoryl chloride (11.5 mmol, 2.0 eq) was taken up in 5 ml of DCM in a 100-ml round-bottom flask fitted with an addition funnel and septum. The solution was blanketed with N_2. In a separate vessel, 3-methyl-1-phenyl-pyrazoline-5-one (5.7 mmol, 1.0 eq) and TEA (17.2 mmol, 3.0 eq) were dissolved in DCM (20 ml). The mixture was transferred to the addition funnel and added drop-wise to the reaction over a 1-hour period. Four hours after the final drop was added, the solvent was removed under vacuum, and the residue was dissolved in saturated aqueous ammonium carbonate (25 ml). After overnight stirring, the solution was washed with DCM, and the aqueous layer was concentrated under vacuum. The residue was taken up in a minimal volume of methanol and purified by preparative HPLC. The appropriate fractions were then pooled, frozen, and lyophilized to give the product 3-methyl-1-phenyl-1H-pyrazol-5-yl phosphate, bis-triethylammonium salt as a white powder, with a yield of 20%.

ALK IHC Scoring Guideline and Statistical Analyses

For assay development and optimization of detections 1 to 5 using *ALK*-positive and -negative NSCLC TMA slides, the intensity of ALK protein immunoreactivity in tumor cells was scored as 0, 1+, 2+, and 3+ by an investigator (H.N.). Because the sample size was small, no statistical analysis was applied to the optimization results.

To further evaluate the performance of detection 3, three blinded pathologists (K.T., A.Y, S.N.H.) scored 80 randomized NSCLC cases (whole-tissue sections) for ALK diagnostic status, using the H-score method.[15] In this method, the percentages of cells with various IHC staining intensities (0, 1+, 2+, or 3+) are quantified so that they sum up to 100%. The H-score is then calculated as follows:

H-score = percentage of 1+ cells + (2 × percentage of 2+ cells) + (3 × percentage of 3+ cells).

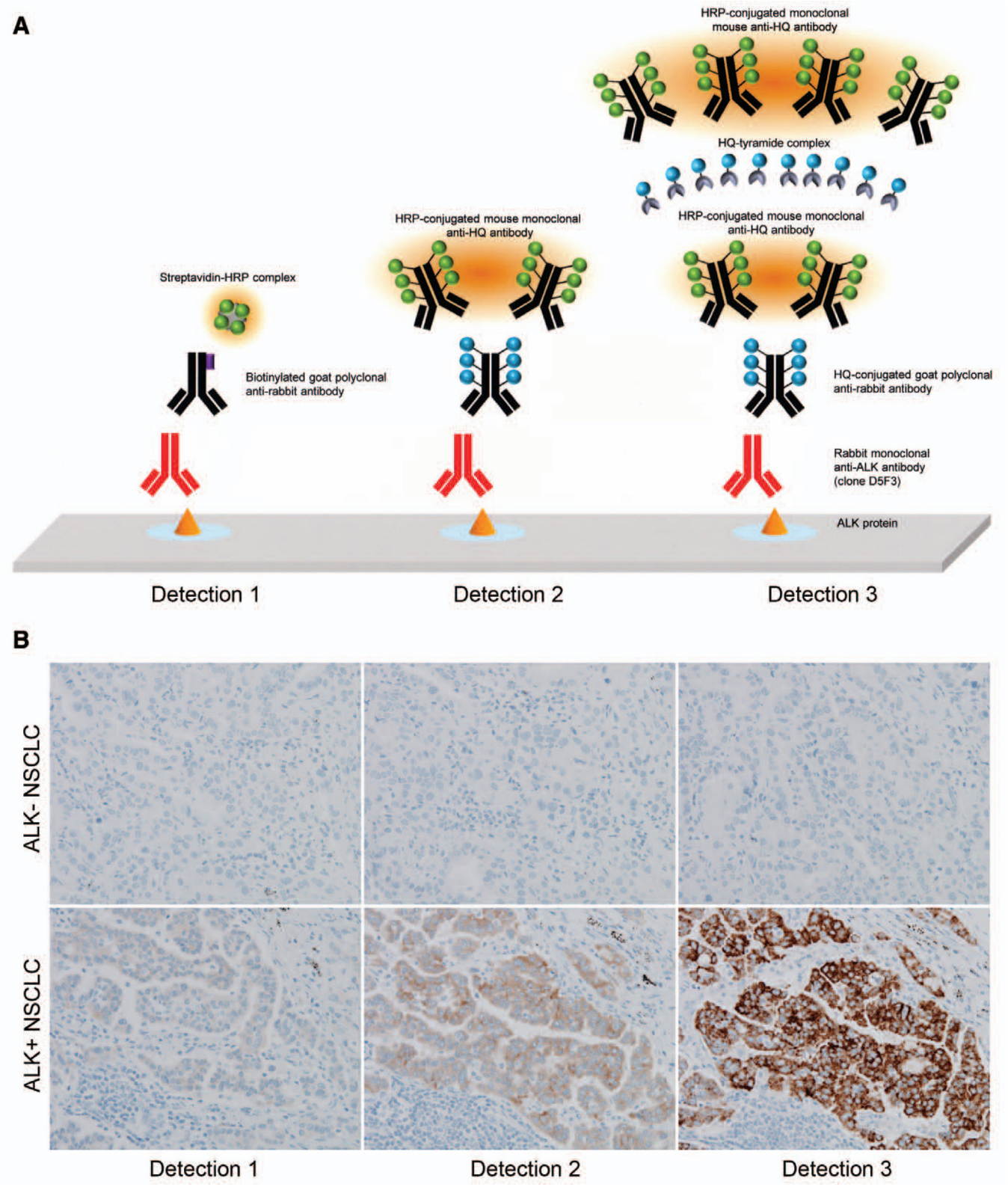

FIGURE 1. Three DAB-based methods for IHC detection of ALK protein. *A*, Schematic diagrams of detections 1, 2, and 3. In all three methods, the target is localized through the HRP-catalyzed deposition of DAB. Detection 1 is a conventional DAB method in which the binding of a biotin-conjugated secondary antibody (black) to the target-bound primary antibody (red) is detected using a streptavidin-HRP complex (green) that binds to the biotin (purple). In detection 2, the IHC signal is amplified through

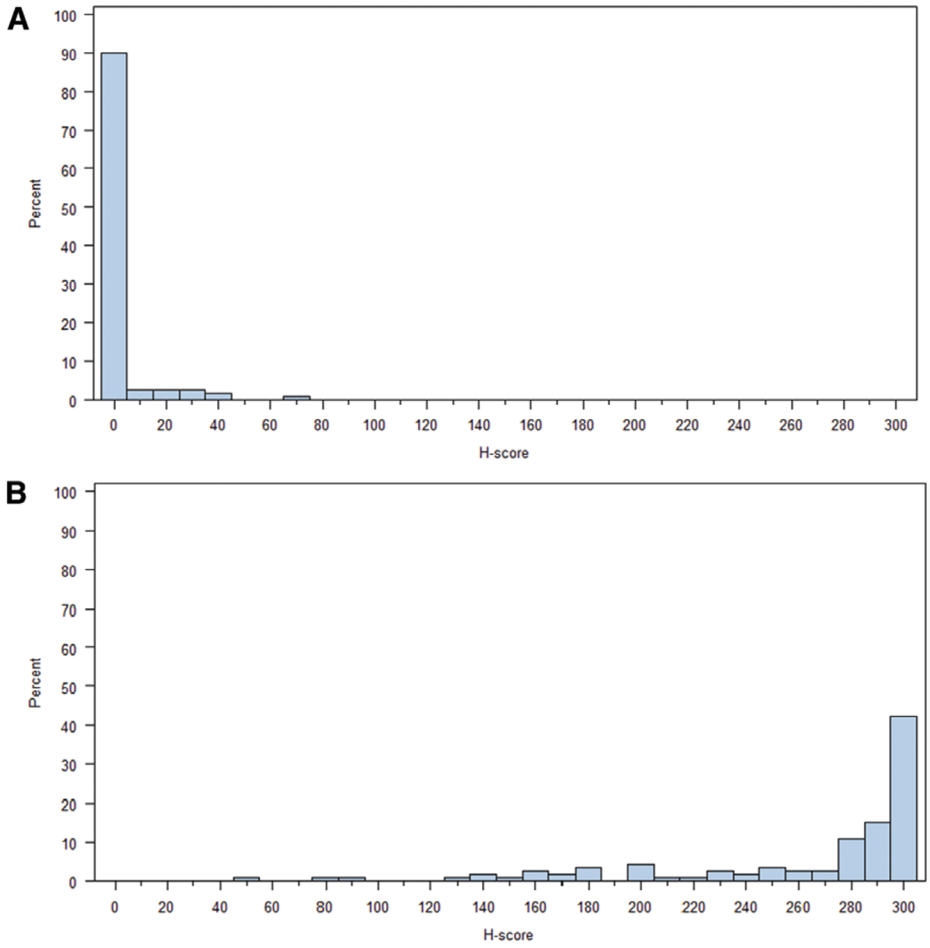

FIGURE 2. Distribution of ALK IHC H-scores in NSCLC cases previously found to be *ALK*-negative (*A*) or *ALK*-positive (*B*) by the Vysis FISH assay. Cases with an H-score of 50 or greater were classified as ALK positive. Ninety percent of the ALK-negative cases had an H-score of 0. ALK, anaplastic lymphoma kinase; IHC, immunohistochemistry; NSCLC, non–small-cell lung cancer.

H-scores can range from 0 to 300. The ALK IHC H-scores for all three readers were compared with the FISH results for each case. The H-score cutoff for ALK positivity was adjusted to maximize the overall agreement between the FISH and IHC results. This cutoff (H-score = 50) was then used to calculate the overall agreement between each reader's IHC and FISH results. Agreement rates for ALK status among readers were also calculated. The data were recorded in Microsoft Excel Spreadsheets, and SAS 9.2 was used for data analysis.

RESULTS

Sensitivity of Three DAB-Based ALK IHC-Detection Methods

To develop a highly sensitive assay for detection of ALK expression in NSCLC tissues, we first examined three DAB-based IHC-detection systems (Fig. 1*A*). The slides used in this analysis contained TMAs of FFPE NSCLC specimens that had been found to be positive or negative for *ALK* gene rearrangement using the Vysis *ALK* FISH assay (14 and 16 tissue cores, respectively).

We used a conventional DAB-based method (detection 1) as a baseline for comparison. In this method, a biotinylated goat antirabbit secondary Ab is bound by a streptavidin-HRP complex. Because tyramide amplification is used to increase IHC assay sensitivity, we next considered improving the detection method by including a tyramide signal amplification system. However, a well-recognized problem in biotinylated tyramide signal amplification is an increase in background staining caused by the presence of endogenous biotin-like molecules.[16] Therefore, in detection 2, we replaced the biotin in our IHC system with a nonendogenous hapten (HQ). The

FIGURE 1. (Continued) the use of a tertiary antibody. The secondary antibody is conjugated to the hapten 3-hydroxy-2-quinoxaline (HQ; blue) rather than biotin, and the anti-HQ tertiary antibody is conjugated to HRP (green). In detection 3, the signal is further amplified using an HQ-conjugated tyramide bridge (gray). *B*, Images of *ALK*-negative (upper row) and *ALK*-positive (lower row) NSCLC cases stained using the three IHC methods (×20) on the same region of the same sample. The *ALK*-negative tissue exhibits no positive staining with any of the three detection systems. The ALK IHC staining signal in the *ALK*-positive samples increases substantially from detection 1 to detection 2 and from detection 2 to detection 3, without a concomitant increase in background staining. ALK, anaplastic lymphoma kinase; DAB, diaminobenzidine; HRP, horseradish peroxidase; IHC, immunohistochemistry; NSCLC, non–small-cell lung cancer.

TABLE 2. Agreement Between ALK Status Results for IHC Versus FISH Assays by Reader

		ALK FISH		
Reader	**ALK IHC[a]**	**Positive**	**Negative**	**Total**
Reader 1	Positive	40	0	40
	Negative	0	40	40
	Total	40	40	80
Reader 2	Positive	40	1	41
	Negative	0	39	39
	Total	40	40	80
Reader 3	Positive	40	0	40
	Negative	0	40	40
	Total	40	40	80

[a]ALK IHC detection 3 method.

HQ was used to amplify the ALK signal without tyramide by attaching it to the goat anti-rabbit secondary Ab and adding an HRP-conjugated anti-HQ Ab. In detection 3, we added the tyramide amplification system to detection 2.

When we compared the ALK protein-detection sensitivity of the two amplified, DAB-based IHC methods (detections 2 and 3) with that of detection 1, a clear difference emerged (Fig. 1*B*). All three detection systems yielded negative staining (IHC intensity score of 0 or <1+) on all 16 NSCLC tissue cores identified as *ALK* negative by the Vysis *ALK* FISH assay. However, of the 14 cores found to be *ALK* positive by the Vysis *ALK* FISH assay, detection 1 yielded negative results for four cores, whereas detections 2 and 3 yielded positive results for 14 cores. Furthermore, whereas detection 2 yielded 3+, 2+, and 1+ staining intensities for 6, 3, and 5 of the *ALK* FISH–positive cores, respectively, detection 3 yielded them for 12, 2, and 0 of the *ALK* FISH–positive cores, respectively. Thus, detection 3 demonstrated the best sensitivity for detecting ALK protein in FFPE NSCLC tissue cores. Furthermore, we observed ALK IHC–negative tumor cells within the whole sections of *ALK* FISH–positive NSCLC cases with detection 2 (data not shown).

Performance Evaluation of the HQ-Tyramide IHC Detection Method

We evaluated the HQ-tyramide IHC detection system (detection 3) by applying it to whole sections of the 40 *ALK* FISH–positive and 40 *ALK* FISH–negative NSCLC cases (Table 1) and having three independent, board-certified

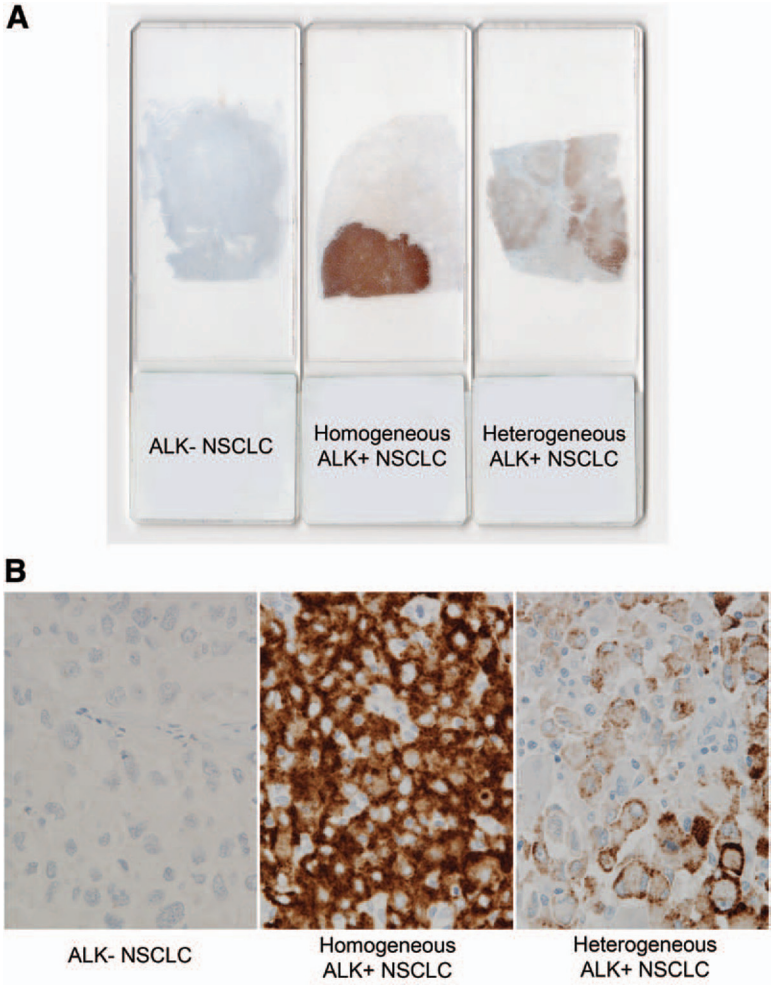

FIGURE 3. Visualization of ALK expression in NSCLC cases using a tyramide-amplified DAB IHC method (detection 3). *A,* Representative nonmagnified images of detection 3–stained NSCLC sections reveal an absence of staining in an *ALK*-negative tumor (left), and homogenous (middle) or heterogeneous (right) staining in two different *ALK*-positive tumors. The homogenous- or heterogeneous-type staining pattern is present throughout the malignant tissue. *B,* Images of detection 3–stained NSCLC sections through a ×60 objective lens. The *ALK*-negative NSCLC cases showed no ALK IHC signal (left). *ALK*-positive NSCLC tissues exhibit homogeneous (middle) or heterogeneous (right) ALK IHC staining. Malignant cells failing to demonstrate ALK IHC staining within an *ALK*-positive tumor were rarely observed. ALK, anaplastic lymphoma kinase; DAB, diaminobenzidine; IHC, immunohistochemistry; NSCLC, non–small-cell lung cancer.

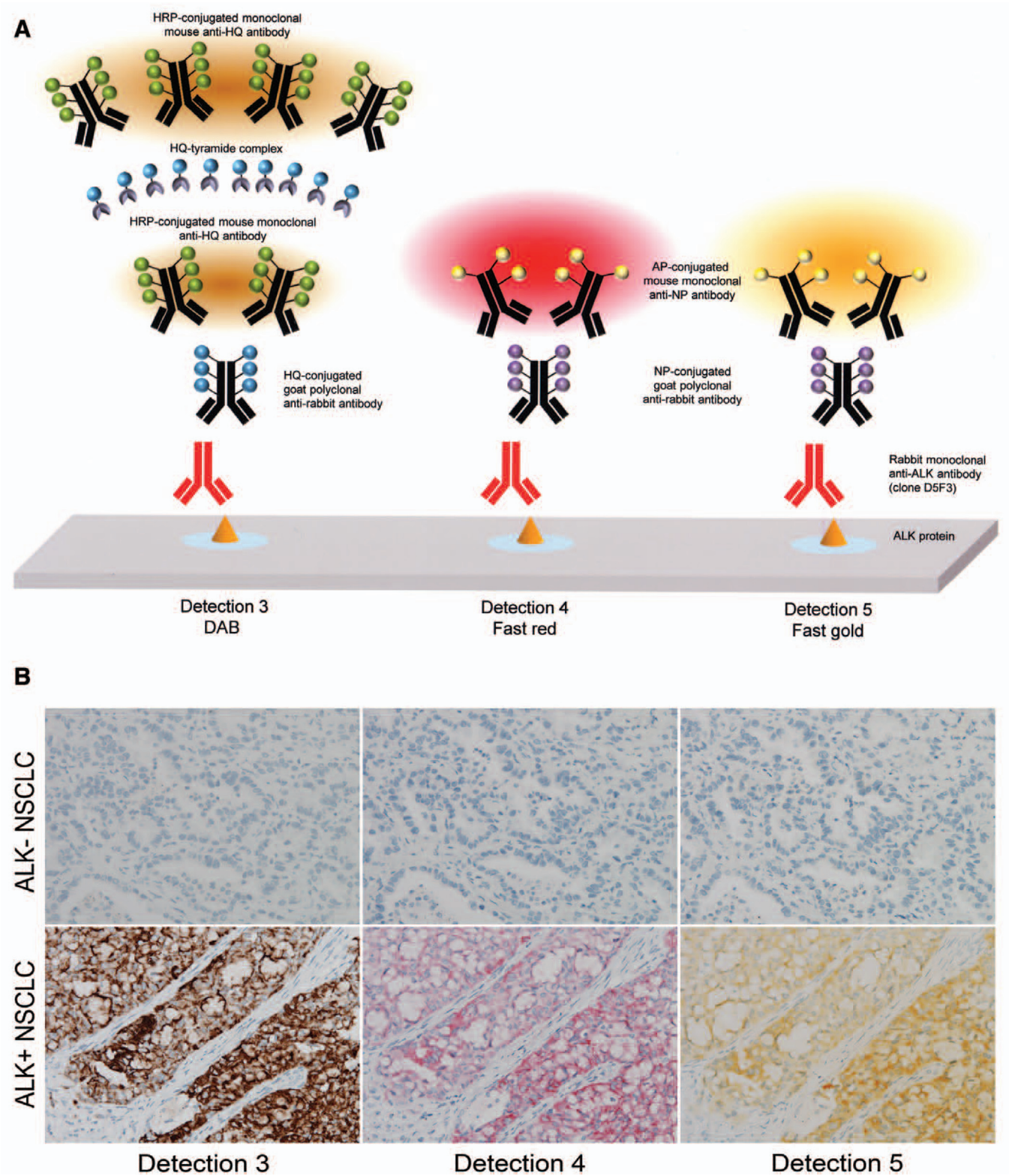

FIGURE 4. Comparison of a tyramide-amplified DAB IHC ALK-detection method (detection 3) with two AP-based IHC ALK-detection methods (detections 4 and 5). *A*, Schematic comparison of the IHC methods. Detection 3, which uses HQ-conjugated, tyramide-amplified IHC detection with HRP-catalyzed deposition of DAB, was used as a control for assay sensitivity. Detections 4 and 5 both use a 5-nitro-3-pyrazole (NP)-conjugated secondary antibody and an AP-conjugated anti-NP antibody. For target visualization, detection 4 uses fast red, whereas detection 5 uses fast gold. *B*, Performance of tyramide-amplified DAB (detection 3; left)

FIGURE 4. (Continued) and AP-based (detections 4 and 5; center and right) ALK IHC methods. None of the methods caused detectable background staining in an *ALK*-negative NSCLC tissue section (top). Relative to tyramide-amplified DAB, AP-based fast red IHC stained *ALK*-positive NSCLC tissue with similar sensitivity but with a wider dynamic range and better resolution (middle). AP-based fast gold IHC staining (right) was similar to AP-based fast red IHC staining (middle) in sensitivity (objective lens, ×20). ALK, anaplastic lymphoma kinase; AP, alkaline phosphatase; DAB, diaminobenzidine; HRP, horseradish peroxidase; HQ, 3-hydroxy-2-quinoxaline; ssIHC, immunohistochemistry; NSCLC, non–small-cell lung cancer.

pathologists familiar with ALK IHC staining evaluate the resulting slides. The slides were randomized and blinded for FISH status before ALK IHC scoring. The pathologists scored the slides using the semiquantitative H-score method[15] described in Materials and Methods section. A threshold H-score value of 50 was selected to maximize the concordance between the results of the Vysis *ALK* FISH assay and the detection 3 IHC assay; cases with an H-score of 50 or greater were classified as ALK IHC positive, and cases with an H-score of less than 50 were classified as ALK IHC negative (Fig. 2).

The readers assigned H-scores of zero for 90% of the *ALK* FISH–negative cases. The IHC interpretations of readers 1 and 3 agreed with the FISH results 100% of the time (score 95% confidence interval, 95.4%–100.0%), whereas interpretations of reader 2 disagreed with the FISH results for one case (98.8% concordance; score 95% confidence interval, 93.3–99.8%; Table 2). All interreader agreement rates were greater than 98%. Only one case was discordant (FISH negative and IHC positive), with an H-score of 70 by one observer.

Differentiated ALK Protein Staining Patterns in NSCLC Visualized by HQ-Tyramide IHC Detection

The ALK IHC status of almost all of the surgical NSCLC cases was visually determinable by the naked eye, but both homogeneous and heterogeneous macroscopic patterns of ALK protein expression were observed (Fig. 3*A*). Twelve ALK IHC–positive cases showed homogeneous macroscopic patterns of ALK staining and 27 ALK IHC–positive cases showed heterogeneous ALK staining. The ALK positivity of one case with weak ALK IHC staining was obvious only under a microscope. Under brightfield microscopic examination, nearly all of the ALK IHC–positive tumor cells exhibited positive staining for ALK protein in those cells morphologically classified as malignant (Fig. 3*B*).

Development of the ALK Gene–Protein Assay

In developing a dual IHC-ISH brightfield assay for *ALK* diagnostic status, we found that combining the DAB-based, HQ-tyramide–amplified IHC system (detection 3) with a brightfield break-apart ISH assay yielded unacceptably dark cytoplasmic DAB staining that obscured the ISH signal (data not shown). Therefore, we sought to develop an alternative IHC detection system for colocalizing ALK protein expression and *ALK* gene rearrangement. Two AP-based systems using the novel hapten NP were developed; as chromogens, detection 4 used fast red, a commonly used AP chromogen, whereas detection 5 used fast gold, a newly developed AP chromogen.

When we compared the tyramide-amplified, DAB-based IHC assay system (detection 3) and the NP-incorporated AP-based systems (detections 4 and 5; Fig. 4*A*), both of the NP systems demonstrated outstanding sensitivity similar to that observed for the tyramide-based DAB IHC system and superior staining resolution and dynamic range on *ALK* FISH–positive TMA slides (Fig. 4*B*). The sensitivity and specificity of detections 4 and 5 were very similar; both detection systems stained *ALK* FISH–positive cases at equivalent and unambiguously positive levels of intensity (2+ or 3+) and yielded no significant staining of tumor cells in any *ALK* FISH–negative cases on TMA slides (Fig. 4*B*).

When we optimized the ALK gene–protein assay using xenograft tumors with known *ALK* status, we found that the optimal procedure combined detection 5 with a subsequent break-apart *ALK* ISH assay (Fig. 5*A*). The optimized procedure produces a gold signal for ALK protein and green and red signals for the 5′ and 3′ *ALK* gene regions, respectively, in *ALK*-positive NSCLC cases. In *ALK*-negative xenograft tumor tissue sections, the proximity of the non–split-apart 5′ and 3′ *ALK* regions superimposed the green and red signals, forming dark brown/black signals, whereas in *ALK*-positive xenograft tumor sections, discrete green and red signals were visible wherever the 5′ and 3′ *ALK* regions were split apart, in addition to superimposed green and red ISH signals (Fig. 5*B*). When used on *ALK*-negative NSCLC tumors, the assay exhibited no immunoreactivity for ALK protein, and the majority of tumor cells showed fused 5′ and 3′ *ALK* ISH signals (Fig. 5*C*, left). When the assay was used on *ALK*-positive NSCLC tumors, both homogeneous staining (consistent ALK immunostaining throughout the tumor area; Fig. 5*C*, top middle) and heterogeneous staining (uneven ALK immunostaining within the tumor area; Fig. 5*C*, top right) were observed, but both staining patterns also demonstrated discrete 5′ and 3′ *ALK* ISH signals in the majority of tumor cells (Fig. 5*C*, bottom middle and right).

DISCUSSION

The most common type of patient specimen used in the clinical diagnostic analysis of patient biomarker status, as well as in basic and medical biomarker research, is the FFPE tissue specimen.[17,18] The clinical analysis typically involves well-established assay methodologies involving IHC, ISH, or PCR.

Crizotinib was FDA-approved for treatment of *ALK*-positive NSCLC patients in 2011, only 4 years after the discovery of *ALK* gene rearrangement in NSCLC[3] and the elucidation of the mechanism by which the rearrangement leads to tumor development.[19] The only FDA-approved *ALK* status testing method is the Vysis *ALK* FISH assay, which is used as companion diagnostic test for identifying patients likely to respond to crizotinib treatment. This test offers two major advantages: it can detect all variants of *ALK* gene rearrangement, and each FISH slide contains an internal control for the

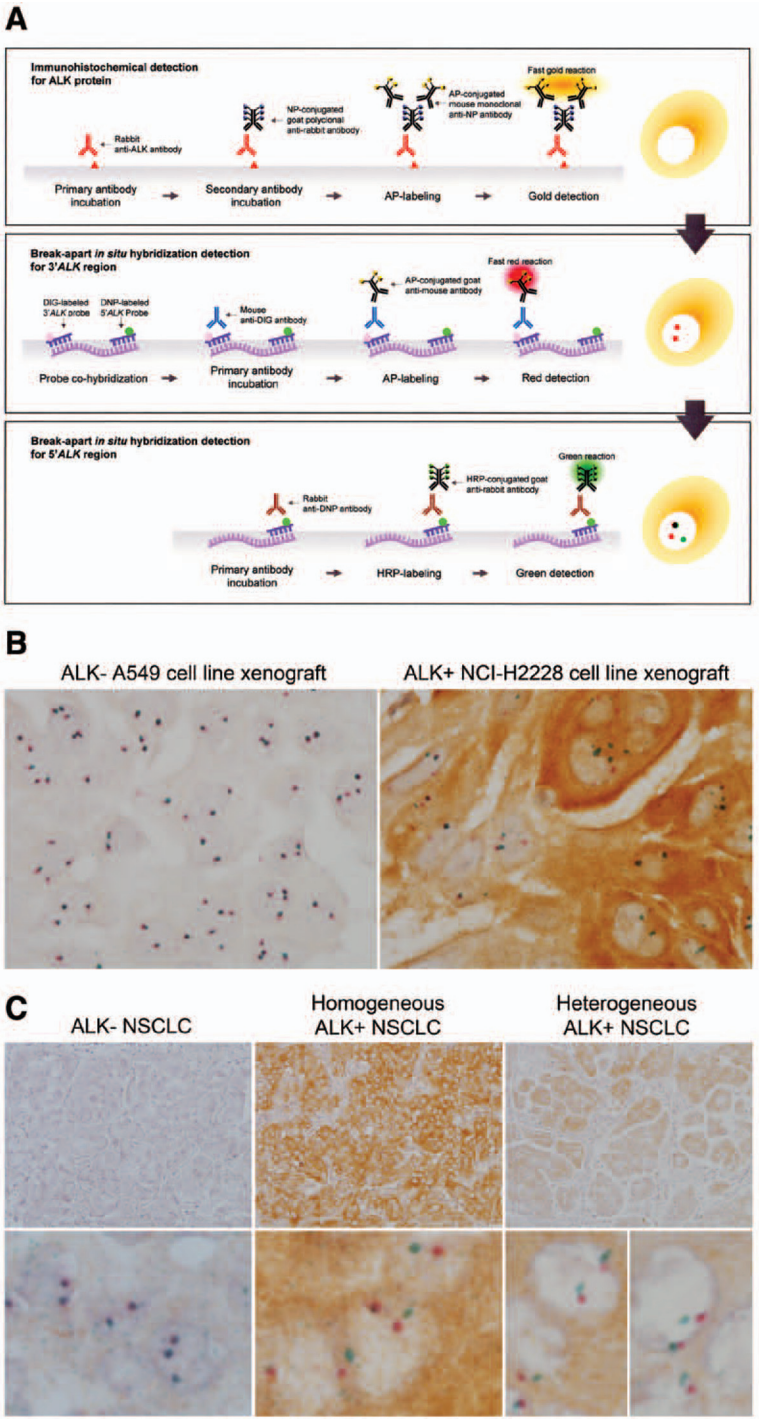

FIGURE 5. Simultaneous detection of ALK protein expression and *ALK* gene rearrangement using the ALK gene–protein assay. *A*, Schematic diagram of the assay. First, ALK protein is stained using detection 5, an IHC method using an NP-conjugated secondary antibody, an AP-conjugated tertiary antibody, and the chromogen fast gold (top). Next, the IHC-stained tissue sections are cohybridized with *ALK* break-apart probes. Binding of the 3′ *ALK* probe is visualized using AP-based ISH with the chromogen fast red (middle). Finally, binding of the 5′ *ALK* probe is visualized using HRP-based ISH with the chromogen HRP-green (bottom). *B*, ALK gene–protein assay staining of xenograft tumors produced from the lung cancer cell lines A549 (*ALK* negative; left) and NCI-H2228 (*ALK* positive; right). In both tumors, wild-type (nonsplit) gene copies appear as dark dots of superimposed red and green signals. In the *ALK*-positive tumor, ALK protein expression is localized by gold staining, and split-apart 5′ and 3′ *ALK* regions appear as discrete green and red dots, respectively. No gold ALK protein signal is visible in the *ALK*-negative tumor (objective lens, ×100). *C*, ALK gene–protein assay staining of NSCLC cases shown with objective lens at ×20 (top) and ×100 (bottom). The gold ALK protein IHC signal is absent in *ALK*-negative cases (left) whereas it is clearly visible in both the homogeneous and heterogeneous *ALK*-positive cases (center and right, respectively). The ISH signals in the *ALK*-negative NSCLC case (bottom left) appear only as superimposed red and green dots, whereas they often appear as discrete green and red dots in both types of *ALK*-positive cases. ALK, anaplastic lymphoma kinase; AP, alkaline phosphatase; HRP, horseradish peroxidase; IHC, immunohistochemistry; ISH, in situ hybridization; NP, 5-nitro-3-pyrazole; NSCLC, non–small-cell lung cancer.

assay performance (fused FISH signals in nontumor cells). However, its utility is limited by the instability of and complex patterns created by FISH signals, by the need for test interpretation training, and its use of fluorescent probe tags requiring specialized equipment for visualization (i.e., a fluorescence microscope). Furthermore, fluorescence visualization compromises the effective recognition of tissue morphology. Therefore, the implementation of *ALK* FISH testing by any clinical laboratory is not an easy task.

Meanwhile, IHC testing for expression of ALK protein in FFPE NSCLC tissue sections[20–26] offers the major advantage that the procedure is relatively simple. However, the low level of ALK protein expressed in *ALK*-positive NSCLC tissue means that the sensitivity and specificity of ALK IHC assay must be carefully optimized for pretreatment method, Ab clone,[20,21,26] and IHC detection system.[20,23] Therefore, the key to successful implementation of the IHC ALK assay as a companion diagnostic test is standardization. Unfortunately,

because normal lung tissues do not express ALK protein at detectable levels, ALK IHC methods lack internal controls, and thus may require control tissues in clinical use. Given the relative advantages and disadvantages of current ALK IHC and *ALK* FISH assays, testing of both types might be required for accurate *ALK* status evaluation of NSCLC patients. In fact, a recent report described a case in which an NSCLC patient specimen tested negative for *ALK* gene rearrangement by FISH but positive for ALK expression by IHC; the patient was effectively treated with crizotinib.[8]

Multiplex RT-PCR methodologies can rapidly and accurately detect known variants of *ALK* fusion genes[7,9] in sputum, bronchial lavage fluid, and pleural effusion samples,[10] and are more sensitive and less subjective than ALK IHC and *ALK* FISH methodologies.[7] However, multiplex RT-PCR is not recommended for clinical use for the detection of *ALK* gene rearrangement in FFPE samples,[6,10] largely because it is difficult to extract high-quality RNA from FFPE tissue sections. In fact, clinical use of a quantitative RT-PCR assay for HER2 testing of FFPE samples raised concern[27] because it yielded unacceptably high false-negative rates (relative to the HER2 IHC and *HER2* FISH methods) in an independent study.[28] Furthermore, RT-PCR–based methods cannot detect as-yet-uncharacterized *ALK* fusion gene variants and do not allow the assessment of biomarker status in the context of tissue morphology.

In our endeavors to develop improved testing methodologies for determining ALK clinical status, we first developed a sensitive HQ-tyramide IHC assay that reproducibly stained ALK protein in FFPE NSCLC tissue sections with low background, revealing both homogeneous and heterogeneous macroscopic patterns of ALK protein expression. Although surgically resected tumors sometimes exhibit immunostaining gradients associated with fixation gradients, the heterogeneity observed for the ALK staining pattern did not seem to be a consequence of fixation heterogeneity. Whereas fixation gradients result from the time required for complete penetration of fixative into a sample and appear as a variation in immunostaining intensity (growing either darker or lighter, depending on the biomarker and detection system) from the center of the sample to its periphery,[29] the heterogeneity observed in our specimens did not present in a typical gradient pattern (Fig. 3*A*), instead appearing intermingled (Fig. 3*B*). Under brightfield microscopic examination, nearly all of the *ALK*-positive samples exhibited positive staining for ALK protein in those cells morphologically classified as malignant. Thus, the heterogeneity seemed to reflect actual variations in the level of *ALK* fusion gene expression in the tumor. Stability differences among various *ALK* fusion gene products[30] might also be a factor in heterogeneous ALK protein staining. Heterogeneity in ALK protein expression or stability could be a confounding factor in slide-based ALK testing, as a small biopsy sample taken from the wrong area of a heterogeneous ALK-positive tumor might not contain enough ALK-positive cells to call positive.

Concurrent or simultaneous assessment of ALK protein expression and *ALK* gene rearrangement in the same tissue section is currently the most promising approach for developing an improved ALK clinical test. However, our initial attempts to combine our HQ-tyramide–amplified IHC method with brightfield break-apart ISH were not successful when one of the ISH probes was labeled with DNP (a frequently used hapten) and DAB was used for IHC detection (data were not shown). An undesired interaction between DAB and DNP produced high background staining. Also, dark cytoplasmic DAB staining of ALK IHC obscured the nuclear ISH signals. Therefore, we sought to develop an ISH-compatible IHC detection system with translucent staining.

We first developed a non–DAB-based, non-tyramide-amplified IHC detection system incorporating AP, NP, and fast red (detection 4). Surprisingly, when compared with the HQ-tyramide DAB IHC detection system (detection 3) in FFPE NSCLC specimens on TMA slides, this system exhibited similar ALK protein detection sensitivity, superior resolution, and a wider dynamic range. Because fast gold, a newly developed chromogen, produces translucent gold staining at AP sites when used with fast blue BB, we created a modified AP-NP IHC system incorporating fast blue BB and fast gold (detection 5). This detection system was similar in ALK sensitivity to the fast red-based system. Fast gold IHC detection was combined with a chromogenic break-apart *ALK* ISH assay that produces red and green signals. The ISH procedure was performed after the IHC procedure because we previously noted that the sensitivity and quality of protein detection in gene–protein assays decreases when ISH is performed before IHC.[31]

When our ALK gene–protein assay was used on tumor sections of xenografts of the ALK-positive lung cancer cell line NCI-H2228, ALK protein expression appeared heterogeneous. Like the HQ-tyramide assay, it produced both homogeneous and heterogeneous staining in different ALK-positive NSCLC cases, suggesting that ALK protein expression might be regulated differentially within a single tumor cell population, leading to heterogeneous expression, or that ALK protein stability might vary among ALK-positive NSCLC cases, resulting in the appearance of heterogeneous expression.

In summary, our explorations of IHC systems for detecting low-level ALK protein expression in NSCLC tissue sections have led to the development of both an HRP-based method using HQ and tyramide amplification and an AP-based method using NP hapten amplification. When combined with a chromogenic break-apart ISH assay, the latter creates a brightfield gene–protein assay that allows covisualization of ALK protein and *ALK* gene rearrangement in FFPE NSCLC tissue sections. This tool for simultaneously assessing both ALK protein expression (IHC) and *ALK* gene rearrangement (ISH) in NSCLC will be valuable for research on the mechanisms driving ALK-dependent malignancies and as a model of new diagnostic approach for identifying patients who might benefit from ALK-targeted therapies. More generally, it also provides proof of concept for the development of new methodologies for the simultaneous assessment of gene structure and protein-expression status in a single cell.

ACKNOWLEDGMENTS

We thank Dr. Koh Furuta and Mr. Susumu Wakai (both from NCCH) for technical assistance; Dr. Nelson R. Alexander, Mr. James G. Grille, and Mr. Stacey Stanislaw (all from Ventana Medical Systems, Inc.) for the ALK probe set;

and Dr. Kyle Kimble (Ventana Medical Systems, Inc.) for critical reviews of the article.

REFERENCES

1. Ong FS, Das K, Wang J, et al. Personalized medicine and pharmacogenetic biomarkers: progress in molecular oncology testing. *Expert Rev Mol Diagn* 2012;12:593–602.
2. Hechtman JF, Polydorides AD. HER2/neu gene amplification and protein overexpression in gastric and gastroesophageal junction adenocarcinoma: a review of histopathology, diagnostic testing, and clinical implications. *Arch Pathol Lab Med* 2012;136:691–697.
3. Soda M, Choi YL, Enomoto M, et al. Identification of the transforming EML4-ALK fusion gene in non-small-cell lung cancer. *Nature* 2007;448:561–566.
4. Cabezón-Gutiérrez L, Khosravi-Shahi P, Diaz-Muñoz-de-la-Espada VM, et al. ALK-mutated non-small-cell lung cancer: a new strategy for cancer treatment. *Lung* 2012;190:381–388.
5. Kwak EL, Bang YJ, Camidge DR, et al. Anaplastic lymphoma kinase inhibition in non-small-cell lung cancer. *N Engl J Med* 2010;363:1693–1703.
6. Thunnissen E, Bubendorf L, Dietel M, et al. EML4-ALK testing in non-small cell carcinomas of the lung: a review with recommendations. *Virchows Arch* 2012;461:245–257.
7. Wallander ML, Geiersbach KB, Tripp SR, et al. Comparison of reverse transcription-polymerase chain reaction, immunohistochemistry, and fluorescence in situ hybridization methodologies for detection of echinoderm microtubule-associated proteinlike 4-anaplastic lymphoma kinase fusion-positive non-small cell lung carcinoma. *Arch Pathol Lab Med* 2012;136:796–803.
8. Sun JM, Choi YL, Won JK, et al. A dramatic response to crizotinib in a non-small-cell lung cancer patient with IHC-positive and FISH-negative ALK. *J Thorac Oncol* 2012;7:e36–e38.
9. Takeuchi K, Choi YL, Soda M, et al. Multiplex reverse transcription-PCR screening for EML4-ALK fusion transcripts. *Clin Cancer Res* 2008;14:6618–6624.
10. Soda M, Isobe K, Inoue A, et al. A prospective PCR-based screening for the EML4-ALK oncogene in non-small cell lung cancer. *Clin Cancer Res* 2012;18:5682–5689.
11. Murakami Y, Mitsudomi T, Yatabe Y. A screening method for the ALK fusion gene in NSCLC. *Front Oncol* 2012;2:24.
12. Nitta H, Zhang W, Kelly BD, et al. Automated brightfield break-apart in situ hybridization (ba-ISH) application: ALK and MALT1 genes as models. *Methods* 2010;52:352–358.
13. Kim H, Yoo SB, Choe JY, et al. Detection of ALK gene rearrangement in non-small cell lung cancer: a comparison of fluorescence in situ hybridization and chromogenic in situ hybridization with correlation of ALK protein expression. *J Thorac Oncol* 2011;6:1359–1366.
14. Yoshida A, Tsuta K, Nitta H, et al. Bright-field dual-color chromogenic in situ hybridization for diagnosing echinoderm microtubule-associated protein-like 4-anaplastic lymphoma kinase-positive lung adenocarcinomas. *J Thorac Oncol* 2011;6:1677–1686.
15. Hatanaka Y, Hashizume K, Nitta K, et al. Cytometrical image analysis for immunohistochemical hormone receptor status in breast carcinomas. *Pathol Int* 2003;53:693–699.
16. Kim SH, Jung KC, Shin YK, et al. The enhanced reactivity of endogenous biotin-like molecules by antigen retrieval procedures and signal amplification with tyramine. *Histochem J* 2002;34:97–103.
17. Klopfleisch R, Weiss AT, Gruber AD. Excavation of a buried treasure–DNA, mRNA, miRNA and protein analysis in formalin fixed, paraffin embedded tissues. *Histol Histopathol* 2011;26:797–810.
18. Shi SR, Shi Y, Taylor CR. Antigen retrieval immunohistochemistry: review and future prospects in research and diagnosis over two decades. *J Histochem Cytochem* 2011;59:13–32.
19. Choi YL, Takeuchi K, Soda M, et al. Identification of novel isoforms of the EML4-ALK transforming gene in non-small cell lung cancer. *Cancer Res* 2008;68:4971–4976.
20. Takeuchi K, Choi YL, Togashi Y, et al. KIF5B-ALK, a novel fusion oncokinase identified by an immunohistochemistry-based diagnostic system for ALK-positive lung cancer. *Clin Cancer Res* 2009;15:3143–3149.
21. Mino-Kenudson M, Chirieac LR, Law K, et al. A novel, highly sensitive antibody allows for the routine detection of ALK-rearranged lung adenocarcinomas by standard immunohistochemistry. *Clin Cancer Res* 2010;16:1561–1571.
22. Paik JH, Choe G, Kim H, et al. Screening of anaplastic lymphoma kinase rearrangement by immunohistochemistry in non-small cell lung cancer: correlation with fluorescence in situ hybridization. *J Thorac Oncol* 2011;6:466–472.
23. McLeer-Florin A, Moro-Sibilot D, Melis A, et al. Dual IHC and FISH testing for ALK gene rearrangement in lung adenocarcinomas in a routine practice: a French study. *J Thorac Oncol* 2012;7:348–354.
24. Park HS, Lee JK, Kim DW, et al. Immunohistochemical screening for anaplastic lymphoma kinase (ALK) rearrangement in advanced non-small cell lung cancer patients. *Lung Cancer* 2012;77:288–292.
25. Paik JH, Choi CM, Kim H, et al. Clinicopathologic implication of ALK rearrangement in surgically resected lung cancer: a proposal of diagnostic algorithm for ALK-rearranged adenocarcinoma. *Lung Cancer* 2012;76:403–409.
26. Conklin CMJ, Craddock KJ, Have C, et al. Immunohistochemistry is a reliable screening tool for identification of ALK rearrangement in non-small-cell lung carcinoma and is antibody dependent. *J Thorac Oncol* 2013;8:45–51.
27. Ignatiadis M, Sotiriou C. Breast cancer: should we assess HER2 status by Oncotype DX? *Nat Rev Clin Oncol* 2012;9:12–14.
28. Dabbs DJ, Klein ME, Mohsin SK, et al. High false-negative rate of HER2 quantitative reverse transcription polymerase chain reaction of the Oncotype DX test: an independent quality assurance study. *J Clin Oncol* 2011;29:4279–4285.
29. Werner M, Chott A, Fabiano, A. et al. Effect of formalin tissue fixation and processing on immunohistochemistry. *Am J Surg Pathol* 2000;24:1016–1029.
30. Heuckmann JM, Balke-Want H, Malchers F, et al. Differential protein stability and ALK inhibitor sensitivity of EML4-ALK fusion variants. *Clin Cancer Res* 2012;18:4682–4690.
31. Nitta H, Kelly BD, Padilla M, et al. A gene-protein assay for human epidermal growth factor receptor 2 (HER2): brightfield tricolor visualization of HER2 protein, the HER2 gene, and chromosome 17 centromere (CEN17) in formalin-fixed, paraffin-embedded breast cancer tissue sections. *Diagn Pathol* 2012;7:60.

